*Inorg. Chem.* **2007**, *46*, 5456–5458


# Resolving the Aluminum Ordering in Aluminosilicates by a Combined Experimental/Theoretical Study of $^{27}$Al Electric Field Gradients

**Xavier Rocquefelte,*,† Frédéric Clabau,† Michael Paris,† Philippe Deniard,† Thierry Le Mercier,‡ Stéphane Jobic,† and Myung-Hwan Whangbo§**

*Institut des Matériaux Jean Rouxel, UMR 6502 CNRS—Université de Nantes, BP 32229, 44322 Nantes Cedex 3, France, RHODIA, Centre de Recherches d'Aubervilliers, 52 rue de la Haie-Coq, 93308 Aubervilliers cedex, France, and Department of Chemistry, North Carolina State University, Raleigh, North Carolina 27695-8204*

Received March 4, 2007

The discrimination between atomic species in light-element materials is a challenging question. An archetypal example is the resolution of the Al/Si ordering in aluminosilicates. Only an average long-range order can be deduced from powder X-ray or neutron diffraction, while magic-angle-spinning NMR provides an accurate picture of the short-range order. The long- and short-range orders thus obtained usually differ, hence raising the question of whether the difference between local and extended orders is intrinsic or caused by the difficulty of obtaining an accurate picture of the long-range order from diffraction techniques. In this communication we resolve this question for the monoclinic phases of $BaAl_2Si_2O_8$ and $SrAl_2Si_2O_8$ on the basis of $^{27}$Al NMR measurements and ab initio simulation of electric field gradient. Although the long- and short-range orders deduced from our XRD and NMR experiments differ, they become similar when the XRD atomic positions are optimized by ab initio electronic structure calculations.

Numerous frameworks of aluminosilicates have a three-dimensional structure based on corner-sharing $AlO_4$ and $SiO_4$ tetrahedra. The Al/Si ordering in these compounds is a result of the reduction of strain and electrostatic energy, which is generally achieved by avoiding the formation of Al−O−Al linkages.[1] This observation has been referred to as the "aluminum avoidance principle". It is often difficult to determine the Al/Si ordering directly by X-ray or neutron diffraction because the $Al^{3+}$ and $Si^{4+}$ cations are very similar in their scattering power. Only an estimation of the average long-range Al/Si order, that is, the relative Al/Si occupancies in their $TO_4$ tetrahedra (T = Al, Si), can be deduced on the basis of their T−O distances.[2−4] In contrast, the $^{29}$Si chemical shift of an aluminosilicate is very sensitive to the local environment, and the short range order can be deduced from peak assignment based on the empirical knowledge of the chemical shifts of the Si atoms tetrahedrally surrounded by 4Al, 3Al + 1Si, 2Al + 2Si, 1Al + 3Si, and 4Si atoms, which are referred to as $Q^4$(4Al), $Q^4$(3Al), $Q^4$(2Al), $Q^4$(1Al), and $Q^4$(0Al), respectively. Nevertheless, these chemical shift ranges are not well separated because of the considerable influence of overall geometric features such as interatomic distances and angles on chemical shift, so that the $^{29}$Si NMR peaks overlap strongly in many complex systems,[5] and an accurate determination of the Al/Si ordering becomes impossible. Similar chemical shift analyses were carried out using other nuclei present in aluminosilicates, that is, $^{17}$O (with enriched compounds) and $^{27}$Al. However, they are quadrupolar nuclei (i.e., nuclei with nuclear spin $I \geq 1$) and interact with the electric field gradients (EFGs) created by the surrounding charges, so that the induced quadrupolar broadening hinders chemical shift analyses. To obtain an NMR spectrum free of the quadrupolar broadening, triple quantum MAS (3QMAS) NMR experiments are carried out, for instance. With this approach, Stebbins et al. were able to estimate the degree of disorder in natural zeolites.[5] Although used with success to show the violation of the "aluminum avoidance" principle in some crystalline and amorphous phases,[6,7] this approach to probing the Al/Si ordering is not easy to carry out because it requires a combination of different NMR experiments and because $^{17}$O-enriched samples are expensive and are not always easy to handle. However, it is important to recognize that EFGs are complementary to chemical shifts and are more sensitive to very small changes in the atomic arrangements surrounding the quadrupolar nuclei beyond the first coordination sphere. Thus,

* To whom correspondence should be addressed. E-mail: xavier.rocquefelte@cnrs-imn.fr.
† Institut des Matériaux Jean Rouxel.
‡ Rhodia.
§ North Carolina State University.

(1) Lowenstein, W. *Am. Miner.* **1954**, *39*, 92−96.
(2) Newnham, R. E.; Megaw, H. D. *Acta Crystallogr.* **1960**, *13*, 303−312.
(3) Chiari, G.; Calleri, M.; Bruno, E.; Ribbe, P. H. *Am. Miner.* **1975**, *60*, 111−119.
(4) Griffen, D. T.; Ribbe, P. H. *Am. Miner.* **1976**, *61*, 414−418.
(5) Stebbins, J. F.; Xu, Z. *Nature* **1997**, *390*, 60−62.
(6) Stebbins, J. F. *Nature* **1987**, *330*, 13−14.
(7) Lee, S. K.; Stebbins, J. F. *Am. Miner.* **1999**, *84*, 937−945.



10.1021/ic7004166 CCC: $37.00 © 2007 American Chemical Society
Published on Web 06/06/2007

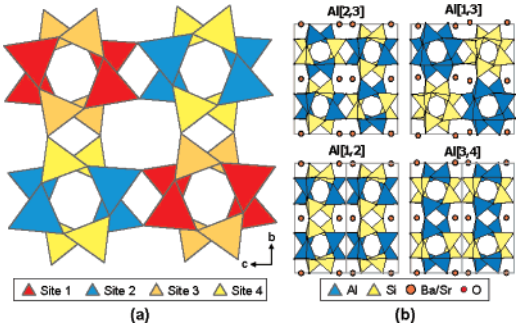


**Figure 1.** Schematic representations of the four different long-range ordered structures for celsian $MAl_2Si_2O_8$ (M = Ba, Sr).

EFGs can be used to probe the Al/Si ordering, once we know how to unambiguously relate EFGs to specific atomic arrangements. Over the past decade, it became possible to accurately calculate the EFGs[8,9] and crystal structures[10] of solids on the basis of ab initio density functional theory (DFT) electronic structure calculations. In the following, we examine the EFGs around the $^{27}Al$ ($I = 5/2$) nuclei in representative aluminosilicates, that is, the monoclinic phases (i.e., the celsian phases) of $BaAl_2Si_2O_8$[11,12] and $SrAl_2Si_2O_8$,[13−16] by combining NMR experiments and DFT electronic structure calculations, and we show that this combined approach is an invaluable tool for probing the Al/Si ordering in aluminosilicates.

The crystal structure of celsian $BaAl_2Si_2O_8$ and $SrAl_2Si_2O_8$ is schematically depicted in Figure 1a, where there are four different tetrahedral sites in which to distribute two Al and two Si atoms. If we consider only the ordered Al/Si arrangements, there are six possibilities. Given the translational symmetry, four of these are unique and are denoted as Al[1,2], Al[1,3], Al[2,3], and Al[3,4] (Figure 1b). Here, the notation Al[*i*,*j*] means that the $Al^{3+}$ ions occupy the sites *i* and *j* and the $Si^{4+}$ ions occupy the remaining two sites. As depicted in Figure 2, the Al atoms of the Al[2,3] structure have only the $Q^4$(4Si) environments, those of the Al[1,2] and Al[3,4] structures only the $Q^4$(3Si) environments, and those of the Al[1,3] structures only the $Q^4$(1Si) environments. Thus, the aluminum avoidance principle is satisfied only for the Al[2,3] structure. Powder XRD measurements do not provide accurate oxygen atom positions, hence leading to a poor description of the oxygen position, affecting the estimation of the long-range order. For example, bond

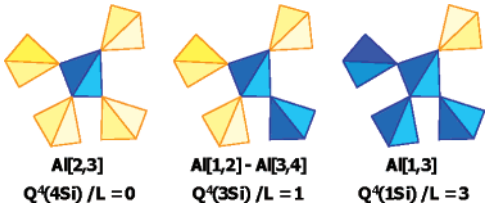


**Figure 2.** Local environment of each $AlO_4$ tetrahedron in the four long-range ordered structural models of $MAl_2Si_2O_8$ (M = Ba, Sr).

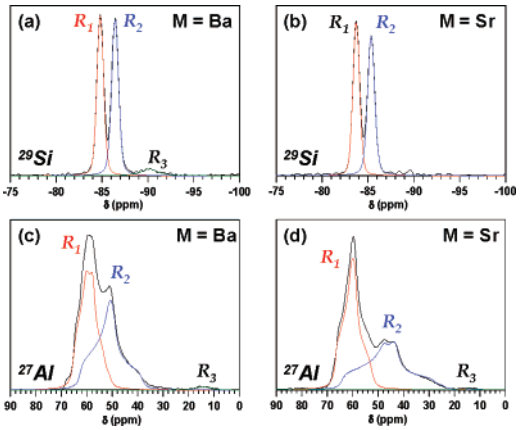


**Figure 3.** $^{29}Si$ and $^{27}Al$ MAS NMR spectra of celsian $BaAl_2Si_2O_8$ and $SrAl_2Si_2O_8$. The decomposed curves for the peaks $R_1$, $R_2$, and $R_3$ are also shown. Only the central transition is observed in $^{27}Al$ MAS NMR spectra.

valence sum[17] calculations for the XRD structure of celsian $SrAl_2Si_2O_8$ show that the oxidation states of the four tetrahedral sites (1, 2, 3, 4) are 3.53, 3.54, 3.58, 3.68, respectively, which suggests that the $Al^{3+}$ ions are randomly distributed.

The $^{29}Si$ and $^{27}Al$ MAS NMR spectra of celsian $BaAl_2Si_2O_8$ and $SrAl_2Si_2O_8$ are presented in Figure 3. The $^{29}Si$ spectra consist of two slightly overlapping peaks ($R_1$ and $R_2$), which are decomposed into two pseudo-Voigt functions with equal integrated intensities and cover almost the total intensity of the spectrum. Similarly, the spectral decomposition of the $^{27}Al$ MAS spectra required only two nonequivalent and equally occupied Al sites leading to the lines $R_1$ and $R_2$. Table 1 summarizes the isotropic chemical shifts ($\delta_{iso}$), the quadrupolar coupling constants ($C_Q$), the asymmetry parameters ($\eta$),[18] and the extracted peak areas. The validity of these decompositions is supported by the $^{27}Al$ 3QMAS spectra shown in Figure S1. For both compounds, only two distinct isotropic chemical shifts in the $^{29}Si$ and $^{27}Al$ NMR spectra are extracted ($R_1$, $R_2$), which correspond to the $Si^{4+}$ ions located at two different $Q^4$(4Al) sites[19,20] and the $Al^{3+}$ ions located at two different $Q^4$(4Si) sites,[21] respectively. It should be noticed that a small broad peak ($R_3$) is also observed in both the $^{29}Si$ and $^{27}Al$ NMR spectra. The $R_3$ $^{29}Si$ peak, at about −90 ppm in celsian $BaAl_2Si_2O_8$, is attributed to $Si^{4+}$ ions at the $Q^4$(3Al) sites.[16] In contrast, the

(8) Blaha, P.; Schwarz, K.; Herzig, P. *Phys. Rev. Lett.* **1985**, *54*, 1192−1195.
(9) Gervais, C.; Profeta, M.; Babonneau, F.; Pickard, C. J.; Mauri, F. *J. Phys. Chem. B* **2004**, *108*, 13249−13253.
(10) Rocquefelte, X.; Boulfelfel, S. E.; Ben, Yahia, M.; Saillard, J-Y.; Halet, J-F. *Angew. Chem., Int. Ed.* **2005**, *44*, 7542−7545.
(11) Clayden, N. J.; Esposito, S.; Ferone, C.; Pansini, M. *J. Mater. Chem.* **2003**, *13*, 1681−1685.
(12) Allameh, S. M.; Sandhage, K. H. *J. Am. Ceram. Soc.* **1997**, *80*, 3109−3126.
(13) Benna, P.; Tribaudino, M.; Bruno, E. *Phys. Chem. Miner.* **1995**, *22*, 343−350.
(14) Töpel-Schadt, J.; Müller, W. F.; Pentinghaus, H. *J. Mater. Sci.* **1978**, *13*, 1809−1816.
(15) Benna, P.; Bruno, E. *Am. Mineral.* **2001**, *86*, 690−696.
(16) Phillips, B. L.; McGuinn, M. D.; Redfern, S. A. T. *Am. Mineral.* **1997**, *82*, 1−7.
(17) Brown, I. D.; Altermatt, D. Acta Cryst. B **1985**, *41*, 244−247.
(18) Pyykkö, E. *Mol. Phys.* **2001**, *99*, 1617−1629.
(19) Dupree, R.; Holland, D.; McMillan, P. W.; Pettifer, R. F. *J. Non-Cryst. Solids* **1984**, *68*, 399−410.
(20) Lippmaa, E.; Magi, M.; Samoson, A.; Tarmak, M.; Engelbardt, G. *J. Am. Chem. Soc.* **1981**, *103*, 4992−4996.
(21) MacKenzie, K. J. D.; Smith, M. E. *Multinuclear Solid-State NMR of Inorganic Materials*; Cahn, R. W., Ed.; Pergamon: New York, 2002.

**Table 1.** Parameters Associated with the $^{29}$Si and $^{27}$Al NMR Spectra of Celsian $BaAl_2Si_2O_8$ and $SrAl_2Si_2O_8$[a]

| | | $BaAl_2Si_2O_8$ | | $SrAl_2Si_2O_8$ | |
|---|---|---|---|---|---|
| | | $R_1$ | $R_2$ | $R_1$ | $R_2$ |
| $^{29}$Si MAS | $\delta_{iso}$ (ppm) | −84.8 | −86.4 | −83.7 | −85.3 |
| | peak area (%)[e] | 47(2) | 48(2) | 51(2) | 49(2) |
| $^{27}$Al MAS | $\delta_{iso}$ (ppm) | 65.4 | 62.6 | 66.9 | 64.4 |
| | peak area (%)[e] | 50(2) | 49(2) | 52(2) | 47(2) |
| | $C_Q$ (MHz) | 4.0 | 5.0 | 3.9 | 6.4 |
| | $\eta$ | 0.62 | 0.92 | 0.83 | 0.78 |
| | $P_Q$ (MHz) | 4.2[b] | 5.7[b] | 4.3[b] | 7.0[b] |
| $^{27}$Al 3QMAS | $\delta_{iso}$ (ppm) | 65.7[c] | 62.9[c] | 66[d] | 63[d] |
| | $C_Q$ (MHz) | 3.8[c] | 4.9[c] | | |
| | $\eta$ | 0.6[c] | 0.9[c] | | |
| | $P_Q$ (MHz) | 4.0[b] | 5.5[b] | 4.1[d] | 7.2[d] |

[a] $C_Q = eV_{ZZ}Q/h$, $\eta = (V_{XX} - V_{YY})/V_{ZZ}$, and $P_Q = C_Q(1 + \eta^2/3)^{1/2}$. $V_{XX}$, $V_{YY}$, and $V_{ZZ}$ are the components of the electric field gradient expressed in its principal axis system with $|V_{ZZ}| \geq |V_{XX}| \geq |V_{YY}|$, and $Q$ is the electric quadrupole moment, which is 146.6 mb for $^{27}$Al. $Q = 0$ for $^{29}$Si because of its nuclear spin $I = 1/2$. [b] Calculated using $C_Q$ and $\eta$ values deduced from the spectral decomposition. [c] Deduced from the spectral decomposition of the 2D 3QMAS spectra. [d] Deduced from the direct reading of the 2D 3QMAS spectra. [e] The remaining peak area corresponds to $R_3$ line, when present.

$R_3$ $^{27}$Al peak, at 14.2 ppm in both the celsian $BaAl_2Si_2O_8$ and $SrAl_2Si_2O_8$ samples, is assigned unambiguously to $Al^{3+}$ ions in octahedral sites.[21] These two additional silicon and aluminum environments may belong to a very small amount of an amorphous impurity phase, not detected by XRD.

In essence, the $^{29}$Si and $^{27}$Al spectra indicate that over the four available sites, two are fully occupied by $Si^{4+}$ ions and the other two by $Al^{3+}$ ions, obeying the aluminum avoidance principle. In addition, the narrowness of the $R_1$ and $R_2$ $^{29}$Si lines indicates a high degree of crystallinity of the prepared sample. The present data agree with the $^{29}$Si spectrum of celsian $SrAl_2Si_2O_8$ by Phillips et al.[16] and with the $^{27}$Al spectrum of celsian $BaAl_2Si_2O_8$ by Clayden et al.[11] However, Clayden et al. misinterpreted their data by using a single Gaussian line shape to simulate the two overlapping $^{27}$Al peaks.

As already mentioned, in relating the EFGs of the $^{27}$Al nuclei to their atomic arrangements, it is necessary to calculate the EFGs on the basis of the crystal structures that are fully optimized by first principles DFT electronic structure calculations. We optimized both the unit cell parameters and the atom positions of celsian $BaAl_2Si_2O_8$ and $SrAl_2Si_2O_8$ for each of the four ordered Al/Si arrangements shown in Figure 1b. As summarized in Tables S1 and S2 of the Supporting Information, the optimized volume of the Al[2,3] structure is very close to that of the XRD structure, and the Al[2,3] structure is the most stable ordered structure. In agreement with the aluminum avoidance principle, the stability decreases in the same order as does the number of Al−O−Al linkages ($L$) per aluminum, that is, Al[2,3] ($L = 0$) > Al[1,2] ($L = 1$) ≈ Al[3,4] ($L = 1$) ≫ Al[1,3] ($L = 3$).

The quadrupolar coupling constants, $C_Q$, and the asymmetry parameters, $\eta$, of the Al sites were calculated for the XRD and for the four optimized ordered crystal structures of celsian $BaAl_2Si_2O_8$ and $SrAl_2Si_2O_8$ using DFT calculations. Table 2 compares the calculated $C_Q$ and $\eta$ values with the experimental values obtained from our $^{27}$Al NMR study.

**Table 2.** Comparison of the Quadrupolar Coupling Constants, $C_Q$ (in MHz), and the Asymmetry Parameters, $\eta$, of the Al Sites in Celsian $BaAl_2Si_2O_8$ and $SrAl_2Si_2O_8$ with the Calculated Values for Their XRD and Optimized Crystal Structures

| | $BaAl_2Si_2O_8$ | | | | $SrAl_2Si_2O_8$ | | | |
|---|---|---|---|---|---|---|---|---|
| | $R_1$ | | $R_2$ | | $R_1$ | | $R_2$ | |
| | $C_Q$ | $\eta$ | $C_Q$ | $\eta$ | $C_Q$ | $\eta$ | $C_Q$ | $\eta$ |
| NMR | 4.0 | 0.62 | 5.0 | 0.92 | 3.9 | 0.83 | 6.4 | 0.78 |
| XRD | −3.70 (Al2) | 0.48 | −13.28 (Al3) | 0.08 | −14.68 (Al3) | 0.23 | −8.41 (Al2) | 0.64 |
| Al[2,3] | 4.08 (Al2) | 0.69 | 5.07 (Al3) | 0.77 | −3.96 (Al3) | 0.98 | 6.97 (Al2) | 0.59 |
| Al[1,3] | 13.86 (Al3) | 0.09 | 13.65 (Al1) | 0.29 | 13.63 (Al3) | 0.07 | 14.30 (Al1) | 0.27 |
| Al[1,2] | −4.89 | 0.74 | −4.89 | 0.74 | 5.66 | 0.91 | 5.66 | 0.91 |
| Al[3,4] | −2.73 | 0.54 | −2.73 | 0.54 | 2.63 | 0.91 | 2.63 | 0.91 |

It should be noted that the Al[2,3] and Al[1,3] structures have two nonequivalent Al sites (space group (SG) = $I2/c$), while the Al[1,2] and Al[3,4] structures have only one (SG = $C2/m$ with the $c$ parameter divided by 2) (Figure 1). Since our $^{27}$Al NMR study shows two nonequivalent Al sites, the Al[1,2] and Al[3,4] structures are inconsistent with experiment, but the Al[2,3] and Al[1,3] structures are not. Table 2 reveals that only the $C_Q$ values of the Al[2,3] ordering are in very good agreement with the experimental $C_Q$ values. Therefore, in terms of both the total energies and $C_Q$ values, celsian $BaAl_2Si_2O_8$ and $SrAl_2Si_2O_8$ are predicted to have the Al[2,3] structure.

Note that the crystal structures of celsian $BaAl_2Si_2O_8$ and $SrAl_2Si_2O_8$ determined from powder XRD are substantially less stable than the corresponding optimized Al[2,3] structures (Table S1) and provide a very poor description of the $C_Q$ values. Bond valence sum calculations using the optimized Al[2,3] structure of celsian $SrAl_2Si_2O_8$ show that the oxidation states of the four tetrahedral sites (1, 2, 3, 4) are 3.94, 3.08, 3.09, 3.93, respectively, as expected for the Al[2,3] structure. Similar results are obtained for $BaAl_2Si_2O_8$. This makes us doubt the conclusion of previous powder XRD studies showing partial disorder in aluminosilicates.

In the probing of the Al/Si ordering in an aluminosilicate on the basis of the EFGs on the Al sites based on $^{27}$Al NMR experiments and first principles DFT calculations, it is necessary to carry out full geometry optimization of its structure. As illustrated in the present study on aluminosilicates and the previous study on borocarbides,[10] it is anticipated that this combined experimental/theoretical approach can resolve many previously intractable questions concerning the local and long range ordering in a wide variety of light-element materials.

**Acknowledgment.** The authors thank Rhodia Electronics & Catalysis for its financial support (Grant 9504213.00) and the CCIPL (Nantes) computing center for computational facilities. M.-H.W thanks the support by the Office of Basic Energy Sciences, Division of Materials Sciences, U.S. Department of Energy, under Grant DE-FG02-86ER45259.

**Supporting Information Available:** Experimental details, Figure S1, and Tables S1 and S2. This material is available free of charge via the Internet at http://pubs.acs.org.

IC7004166